A CFD ANALYSIS OF THE OPERATING CONDITIONS AND GEOMETRY EFFECTS ON THE PERFORMANCE OF A SUPERSONIC GAS EJECTOR

Thaís Piva de Castro, tha.piva@gmail.com
Edson Luiz Zaparoli, zaparoli@ita.br
Cláudia Regina de Andrade, claudia@ita.br
Instituto Tecnológico de Aeronáutica, Departamento de Engenharia Aeronáutica e Mecânica, Área de Aerodinâmica, Propulsão e Energia – Praça Marechal Eduardo Gomes, 50, Vila das Acácias, CEP 12.228-900, São José dos Campos, SP, Brasil.

Abstract. *Supersonic ejectors are widely used in different applications such as aerospace, propulsion and refrigeration. The ejector is characterised by the use of the kinetic energy of one fluid stream (the primary fluid) to drive a second fluid stream (the secondary fluid) by direct mixing. An ejector is a simple device since that it consists of four main unmoving components: primary nozzle, secondary inlet, mixing chamber and diffuser. This type of device is attractive due the lack of moving parts, low cost and high reliability. The performance of a gas driven supersonic ejector depends upon its geometry (shape, layout and dimensions), the properties of the gas and secondary fluid (density, molecular weight and specific heat ratios), the flow conditions (pressures, temperatures, mass flow rates) at the primary and secondary inlets and the diffuser outlet. Although the gas driven ejector is conceptually a simple device, the physical processes that occur in flow are extremely complex. In this work was done the numerical analyze the gas/gas supersonic ejector performance under the followings conditions: (i) the constant pressure mixing chamber length and mass flow at secondary inlet in the (ii) CPM and (iii) CAM ejectors. The mathematical model of this compressible flow was numerically solved using finite volume method with a coupled density-based approach. An adaptive mesh refinement was employed to capture shock reflections and shock-mixing layer interaction. The simluation results shows that the increase pressure was reduced when the mass flow in second inlet was increased.*

Keywords*: CFD, ejector, supersonic, geometry, compressible*

1. INTRODUCTION

The ejector was invented by Sir Charles Parsons around 1901, and in 1910 an ejector was used by Maurice Leblanc in the first steam jet refrigeration system. An ejector is a simple device since that it consists of four main unmoving components: primary nozzle, secondary inlet, mixing chamber and diffuser, Fig .1, and is widely used in different applications such as aerospace, propulsion and refrigeration. This type device is attractive due to lack of moving parts, low cost and high reliability.

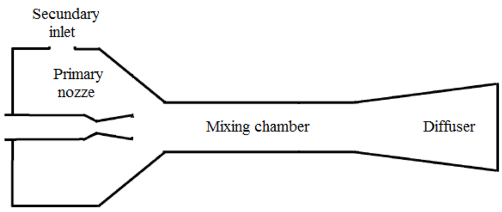

Figure 1. Ejector configuration

The ejector design can be classified into two types according to the position of the primary nozzle. The ejector, which has the nozzle with its exit plane located within the divergent section the mixing chamber, in front of the constant area section, as described by Keenan's theory, the static pressure was assumed to be constant through the mixing process. Therefore, this kind of ejector is known as a 'constant pressure mixing ejector' (CPM), ("Fig. 2a"). For the nozzle with its exit located within the constant area section, the ejector is called a 'constant area mixing ejector' (CAM), ("Fig. 2b"), Keenan et al. (1950) and Rusly et al. (2002).

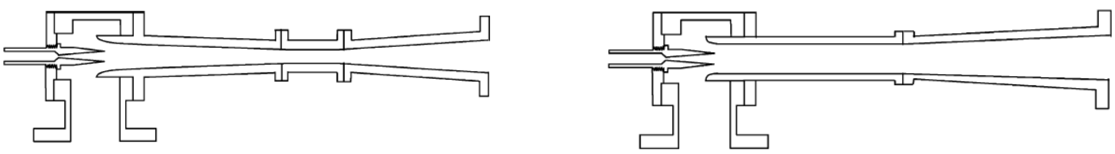

(a) (b)

Figure 2. The ejector configuration: (a) CPM e (b) CAM, Chunnanond and Aphornratana (2004a)

Bartosiewicz et al. (2005) performed numerical and experimental investigations to obtain a reliable hydrodynamics model of a supersonic ejector for refrigeration application. In the first part of their work, the performance of six turbulence models is evaluated in terms of correct representation of physical phenomena for supersonic ejectors, in the second part, the tested model was used to simulate the different operation modes of a supersonic ejector, ranging from on-design point to off-design. The work showed that the RNG and sst - $k-\omega$ models were the best suited to predict the shock, strength, and the mean line pressure recovery. However, the sst - $k-\omega$ model has shown better performances in term of stream mixing. In another study Bartosiewicz et al. (2006) used the CFD modeling to study the flow structure and operation under various operating conditions. This was the first paper dealing with local CFD modeling that takes into account shock–boundary layer interactions in a real refrigerant. The numerical results obtained, contribute to understanding the local structure of the flow and demonstrate the crucial role of the secondary nozzle for the mixing rate performance. They concluded that entrainment performance is mainly built in the secondary nozzle, while recompression is achieved in the mixing chamber. They concluded also that the strong shocks waves occurring at the secondary nozzle exit can dramatically decrease the mixing rate and even reverse the flow and the CFD software can predict ejector malfunction.

Sriveerakul et al. (2007a) presented a CFD analysis in order to predict the performance of a steam ejector used in refrigeration applications. This study was reported in two papers. The first, Sriveerakul et al. (2007a), presented an investigation on the effects of operating conditions and geometries on steam ejector and, in the second, Sriveerakul et al. (2007b), concentrated on the use of CFD in visualizing the change in the flow structure and the mixing process inside the steam ejector as influenced by interested parameters, ejector's operating conditions and geometries. The CFD visualization shows two series of oblique shocks. The first series was found immediately after the primary fluid stream leaves the primary nozzle and begins to mix with the secondary fluid stream. The second series of oblique shock was found at the beginning of the diffuser section as a result of a non-uniform mixed stream. It can be seen that both entrainment ratio and critical back pressure can be varied simultaneously by adjusting three parameters, the primary fluid saturated pressure, the secondary fluid saturated pressure, and the primary nozzle size.

Yinhai et al. (2009) presented a Computational Fluid Dynamics (CFD) analysis the effects of two important ejector geometry parameters: the primary nozzle exit position (NXP) and the mixing section converging angle h, on its performance. The author created 95 different ejector geometries and tested under different working conditions. From 210 testing results, it is found that the optimum NXP is not only proportional to the mixing section throat diameter, but also increases as the primary flow pressure rises. On the other hand, the ejector performance is very sensitive to h, especially near to the optimum working point. A relatively bigger h is required to better maximize the ejector performance when the primary flow pressure rises.

This work presents a numerical study about supersonic gas ejector based on geometric parameters provided by Bartosiewicz et al. (2005) and Desevaux (2001). The mathematical model is numerically solved (continuity, momentum, energy and sst$-k-\omega$ turbulence model) using finite volume method. The validation procedure is performed testing the performance of different turbulence models (realizable – $k-\varepsilon$ or sst – $k-\omega$). It is also studied the advectives terms treatment (first and second order upwind discretization schemes). These preliminary results were presented in Castro (2010). After, the ejector performance is analyzed under the followings conditions: (i) the constant pressure mixing chamber length and mass flow at secondary inlet in the (ii) CPM and (iii) CAM ejectors.

2. PROBLEM DEFINITION

In the ejector, "Fig. 3", the primary fluid a high pressure and temperature expands and accelerates through the primary nozzle convergent-divergent (i), reaches sonic velocity in the throat and is ejected with supersonic velocity to create a very low pressure region at the primary nozzle exit (ii) and subsequently in the mixing chamber. This means "a secondary fluid" can be entrained into the mixing chamber. The speed of the secondary fluid rises to sonic value (iii) and chokes. Then the mixing process begins. This mixing causes the primary flow to be retarded whilst secondary flow is accelerated. By the end of the mixing chamber, the two streams are completely (iv). Due to a high pressure region downstream of the mixing chamber's throat, a normal shock of essentially zero thickness is induced (v). This shock causes a major compression effect and a sudden drop in the flow speed from supersonic to subsonic. A further compression of the flow is achieved (vi) as it is brought to stagnation through a subsonic diffuser.

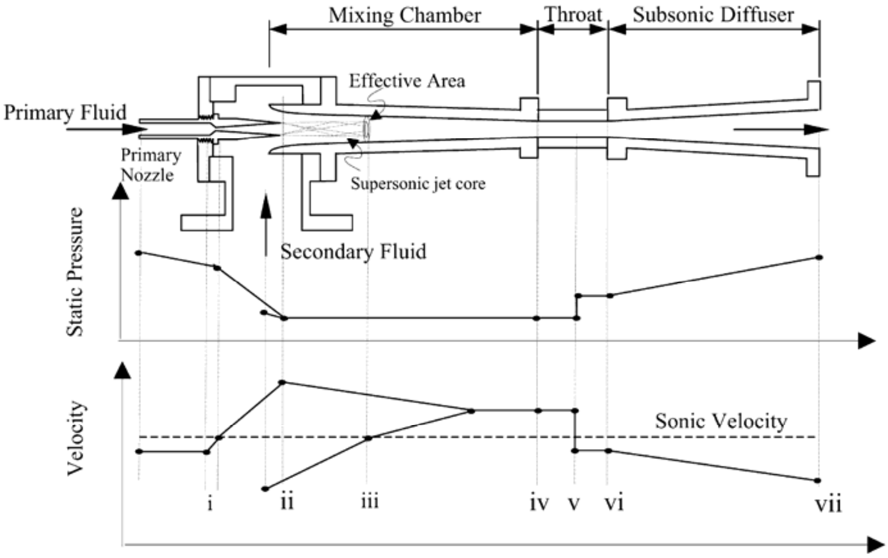

Figure 3. Schematic view and the variation of stream pressure and velocity as a function of location along an ejector, Sriveerakul et al. (2007a).

3. MATHEMATICAL MODELING

The mathematical formulation can be described, in cartesian form, by continuity, momentum, energy and turbulence model equations (sst – k– ω), Eqs. (1) to (6), respectively. Following assumptions were taken into account: two dimensional, axisymmetrical, compressible, ideal gas, air flow, unsteady state regime and constants transport properties.

Continuity equation

$$\frac{\partial \rho}{\partial t}+\frac{\partial}{\partial x_i}(\rho u_i)=0 \tag{1}$$

Momentum equation

$$\frac{\partial}{\partial t}(\rho u_i)+\frac{\partial}{\partial x_j}(\rho u_i u_j)=-\frac{\partial P}{\partial x_i}+\frac{\partial \tau_{ij}}{\partial x_j} \tag{2}$$

where stress tensor components are evaluated as:

$$\tau_{ij}=\left(\mu+\mu_t\right)\left(\frac{\partial u_j}{\partial x_i}+\frac{\partial u_i}{\partial x_j}\right)-\frac{2}{3}\left(\mu+\mu_t\right)\frac{\partial u_k}{\partial x_k}\delta_{ij}$$

Energy equation

$$\frac{\partial}{\partial t}(\rho E)+\frac{\partial}{\partial x_j}(u_j(\rho E+P))=\frac{\partial}{\partial x_j}\left[\Gamma_E\frac{\partial T}{\partial x_j}+u_i\left(\tau_{ij}\right)\right] \tag{3}$$

Equations of the sst - k– ω model

$$\frac{\partial}{\partial t}(\rho k)+\frac{\partial}{\partial x_i}(\rho k u_i)=\frac{\partial}{\partial x_j}\left[\left(\mu+\frac{\mu_t}{\sigma_k}\right)\frac{\partial k}{\partial x_j}\right]+\tilde{G}_k-Y_k \tag{4}$$

$$\frac{\partial}{\partial t}(\rho\omega)+\frac{\partial}{\partial x_i}(\rho\omega u_i)=\frac{\partial}{\partial x_j}\left[\left(\mu+\frac{\mu_t}{\sigma_\omega}\right)\frac{\partial\omega}{\partial x_j}\right]+G_\omega-Y_\omega \tag{5}$$

The constant values of the sst - $k-\omega$ model used in this work are: $\sigma_{k,1}=1.176$; $\sigma_{k,2}=1.0$; $\sigma_{\omega,1}=2.0$; $\sigma_{\omega,2}=1.168$; $\alpha^*_\infty=1$; $R_k=6$; $\beta_i=0{,}072$;

The turbulent viscosity is computed from:

$$\mu_t=\frac{\rho k}{\omega}\frac{1}{\max\left[\frac{1}{\alpha^*},\frac{SF_2}{a_1\omega}\right]} \tag{6}$$

where

$$\sigma_k=\frac{1}{F_1/\sigma_{k,1}+(1-F_1)/\sigma_{k,2}};\ \sigma_\omega=\frac{1}{F_1/\sigma_{\omega,1}+(1-F_1)/\sigma_{\omega,2}};$$

$$\alpha^*=\alpha^*_\infty\left(\frac{\alpha^*_0+R_{e_t}/R_k}{1+R_{e_t}/R_k}\right);\ R_{e_t}=\frac{\rho k}{\mu\omega};\ \alpha^*_0=\frac{\beta_i}{3};$$

$$F_1=\tanh\left(\phi_1^4\right);\ F_2=\tanh\left(\phi_2^2\right)$$

$$\phi_1=\min\left[\max\left(\frac{\sqrt{k}}{0.09\omega y'},\frac{500\mu}{\rho y^2\omega}\right),\frac{4\rho k}{\sigma_{\omega,2}D^+_\omega y^2}\right];\ \phi_2=\max\left(\frac{\sqrt{k}}{0.09\omega y'},\frac{500\mu}{\rho y^2\omega}\right)$$

$$D^+_\omega=\max\left[2\rho\frac{1}{\sigma_{\omega,2}}\frac{1}{\omega}\frac{\partial k}{\partial x_j}\frac{\partial\omega}{\partial x_j},10^{-10}\right];$$

Table 1. Nomenclature.

$\tilde{G}_k$;	generation of turbulence kinetic energy due to the mean velocity gradients
G_ω;	represents the generation of ω
P;	Pressure
T;	Temperature
Y_k and Y_ω;	dissipation of k and ω due to turbulence
k;	turbulence kinetic energy
v;	kinematic viscosity
μ;	molecular dynamic fluid viscosity
ρ;	fluid density
μ_t;	turbulent dynamic fluid viscosity
ω:	specific dissipation rate
σ_k and σ_ω;	turbulent Prandtl numbers for (k) and (ω), respectively
$\Gamma_E=\Gamma+\Gamma_T$;	effective thermal conductivity
i, j, k;	space components

Boundary conditions

In this work, the geometrical configuration of the computational domain of a constant pressure supersonic ejector was done according to the experimental setup of Bartosiewicz et al. (2005) and Desevaux (2001), shown in "Fig. 4".

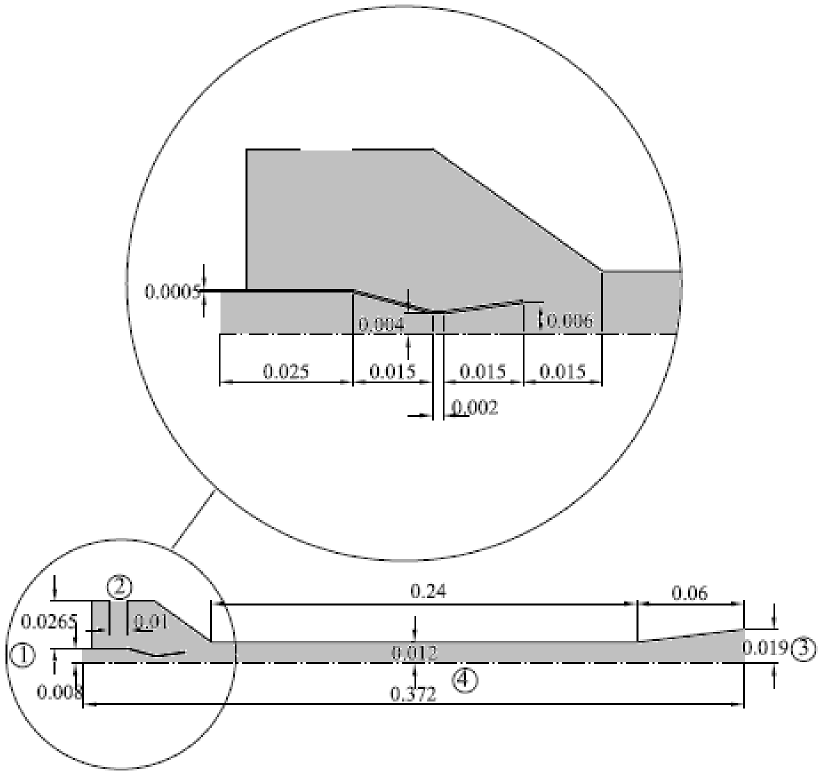

Figure 4. Geometric parameters of the constant pressure supersonic ejector (dimensions in m).

At surface 1, Fig. (4), or primary fluid inlet, the total pressure and total temperature, and normal flow direction to input surface are prescribed. At surface 2, secondary fluid inlet, total temperature and mass flow rate are prescribed, and in the surface 3, or exit, the static pressure is imposed. At all inlet boundaries, 5% for turbulent intensity and 5 for turbulent viscosity ratio are specified, while, axisymmetrical boundary condition is prescribed at surface 4. All the walls are considered to be adiabatic with no slip and enhanced wall law are used as turbulence model boundary conditions. Numerical values for inlet and outlet boundary conditions are shown in Tab. (2).

Table 2. Surfaces, boundary condition type, boundary conditions and values.

Surfaces	Boundary condition type	Prescribed Boundary Values	
1	Pressure inlet	T_{Total} = 300 K	P_{Total} = 4 atm
2	Mass flow rate	T_{Total} = 300 K	$\dot{m}$ = 0.020; 0.024; 0.028; 0.030; 0.032; 0.036; 0.040; 0.044; 0.048 kg/s
3	Pressure outlet	T_{Total} = 300 K	P_{static} = 1 atm

4. COMPUTATIONAL STRATEGY

The numerical simulations have been performed using the commercial CFD package FLUENT (12.1), Fluent (2008), based on finite volume methods (FVM). The compressible, turbulent, axisymmetric, steady state flow was calculated using a pseudo-transient technique with a density based approach**.** The turbulence model utilized was sst –k – ω. The transient formulation was first order implicit. The numerical approximation utilized was first order for the advective terms and pressure. During algebraic equations system iterative solution, CFL is set to 1.

5. RESULTS

On the simulations, the domain shown in Fig. 4 was used, which is based on the geometric parameters of Bartosiewicz et al. (2005) and Desevaux (2001).

In order to find out the optimum length of the constant pressure mixing chamber, 7 ejectors, in a total of 28 cases, were studied by varying of length of mixing chamber and mass flow on secondary inlet. The mass flow on secondary inlet ranges from 0.02 to 0.032 kg/s and the pressure inlet remains at 4 atm.

Figure 5 shows variation of the length of constant pressure mixing chamber with the pressure difference between outlet and secondary inlet. The results indicate that the parameter length of mixing chamber is of critical importance to the ejector performance and should be carefully designed inside the optimum range. In these testes, for the ejector modeling, the optimum length is found in the range of 1.8 and 2.2 m, being that the lower mass flow in the secondary inlet greater the pressure difference (P_3-P_2) and thus produces better performance.

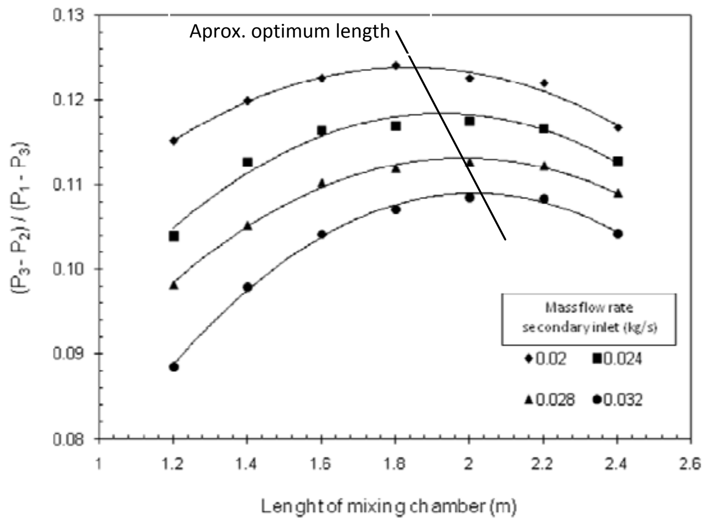

Figure 5. Analysis of constant pressure mixing chamber length

To evaluate mass flow in the secondary inlet in the constant pressure mixing chamber supersonic ejector performance, a simulation ranging the mass flow in the secondary inlet was performed. These results were shown in Fig. (6). It is possible to see a reduction in the pressure increase (P_3-P_2) as consequence of mass flow rate increases in the secondary inlet. Thus, the lower the mass flow in the secondary inlet, greater the pressure difference resulting in better performance.

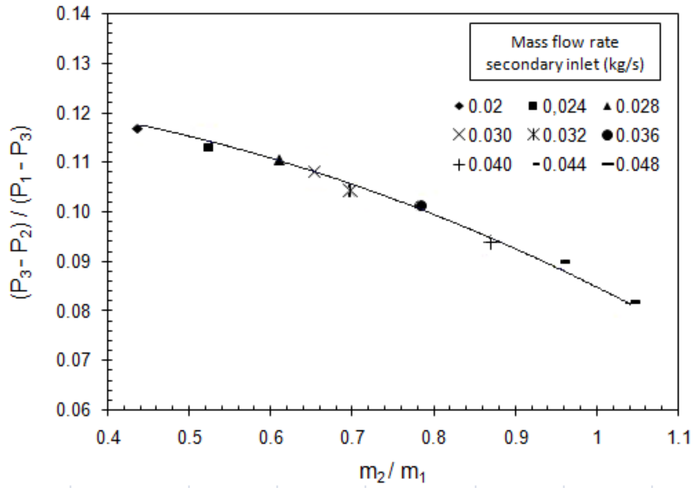

Figure 6. Analysis of mass flow in the secondary inlet of constant pressure mixing chamber

To evaluate mass flow in the secondary inlet in the constant area mixing chamber supersonic ejector performance, a simulation ranging the mass flow in the secondary inlet was performed. These results were shown in Fig. (7) It is possible to see a reduction in the pressure increase (P_3-P_2) as consequence of mass flow rate increases in the secondary inlet. Thus, the lower mass flow in the secondary inlet, greater the pressure difference resulting in better performance.

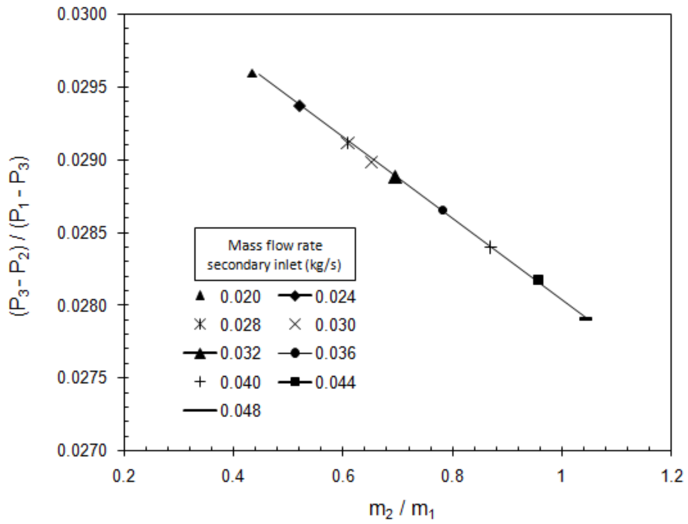

Figure 7. Analysis of mass flow in the secondary inlet of constant area mixing chamber

6. CONCLUSION

In this work it was performed a numerical simulation to analyze the performance of gas supersonic ejector, varying followings conditions: (i) the constant pressure mixing chamber length and mass flow at secondary inlet in the (ii) CPM and (iii) CAM ejectors.

The validation procedure performed testing the performance of different turbulence models and advectives terms treatments are presented in Castro (2010).

In the tested, for the ejector modeling, the optimum length of constant pressure mixing chamber is found in the range of 1.8 and 2.2 m. Being that the lower mass flow in the secondary inlet greater the pressure difference (P_3-P_2) and thus better performance.

The analysis the mass flow on the secondary inlet showed the lower mass flow on the secondary inlet, greater the pressure difference between the secondary inlet and outlet resulting in a better performance, for the two models the ejectors. Being that the CPM ejector presents better performance that the CAM ejector.

7. ACKNOWLEDGEMENTS

The authors would like to acknowledge the CAPES by the financial support and the GSET (Group of Simulation of Flow and Heat Transfer) by the computational support.

8. REFERENCES

Bartosiewicz, Y., Aidoun, Z., Desevaux, P. and Mercadier, Y., 2005, ”Numerical and experimental investigations on supersonic ejectors” , Int. J. of Heat and Fluid Flow, Vol. 26, pp. 56-70.

Bartosiewicz, Y., Aidoun, Z. and Mercadier, Y., 2006, “Numerical assessment of ejector operation for refrigeration applications based on CFD”, Applied Thermal Engineering, Vol. 26, pp. 604-612.

Castro, T.P., Lima, R.C., Ribeiro, L.N., Zaparoli, E.L. and Andrade, C.R., 2010, “A CFD Analysis of Gas-Flow in a Supersonic Ejector”, CONEM 2010.

Chunnanond, K. and Aphornratana, S., 2004a, “Ejectors: applications in refrigeration technology”, Renewable and Sustainable Energy Reviews, Vol. 8, pp. 129-155.

Desevaux, P., 2001, “A method for visualizing the mixing zone between two co-axial flows in an ejector”, Optics and Lasers in Engineering, Vol. 35, pp. 317-323.

FLUENT INC. User’s guide, versão 12.0, 2008. Disponível em <www.fluent.com>. Acesso em 25 de maio. 2010.

Keenan, J.H., Neumann, E.P. and Lustwerk, F., 1950, “An investigation of ejector design by analysis and experiment”, ASME J. Appl. Mech. Trans., Vol.72, pp.299–309.

Rusly, E., Aye, L., Charters, W.W.S., Ooi, A. and Pianthong, K., 2002, “Ejector CFD modeling with real gas model”, Mechanical Engineering Network of Thailand the 16th Conference, pp.150–5.

Sriveerakul, T., Aphornratana, S. and Chunnanond, K., 2007a, “Performance prediction of steam ajector using computational fluid dynamics: Part 1. Validation of the CFD results”, Int. J. of Thermal Sciences, Vol. 46, pp. 812-822.

Sriveerakul, T., Aphornratana, S. and Chunnanond, K., 2007b, “Performance prediction of steam ajector using computational fluid dynamics: Part 2. Flow structure of a steam ejector influenced by operating pressures and geometries”, Int. J. of Thermal Sciences, Vol. 46, pp. 823-833.

Yinhai, Z., Wenjian, C., Changyun, W. and Yanzhong, L., 2009, “ Numerical investigation of geometry parameters for design of high performance ejectors”, Applied Thermal Engineering, Vol. 29, pp. 898-905.

9. RESPONSIBILITY NOTICE

The author(s) is (are) the only responsible for the printed material included in this paper.